nature communications

Article

https://doi.org/10.1038/s41467-024-54328-5

Tailored chiral phosphoramidites support highly enantioselective Pd catalysts for asymmetric aminoalkylative amination

Received: 17 July 2024

Accepted: 8 November 2024

Published online: 02 December 2024

Check for updates

Suchen Zou[1,3], Zeyu Zhao[1,3], Guoqing Yang[1] & Hanmin Huang[1,2]

Even though tuning electronic effect of chiral ligands has proven to be a promising method for designing efficient catalysts, the potential to achieve highly selective reactions by this strategy remains largely unexplored. Here, we report a palladium-catalyzed enantioselective ring-closing aminoalkylative amination of aminoenynes enabled by rationally tuning the remote electronic property of 1,1′-binaphthol-derived phosphoramidites. With a tailored 6,6′-CN-substituted 1,1′-binaphthol-derived phosphoramidite as a ligand, a broad range of aromatic amines are compatible with this reaction, allowing the efficient synthesis of a series of enantioenriched exocyclic allenylamines bearing saturated *N*-heterocycles with up to >99% enantiomeric excess. Remarkably, a one-pot aminoalkylative amination/hydroamination process for the rapid synthesis of chiral spirodiamines promoted by this catalytic system is also established. Detailed mechanistic studies provide solid evidence to support that the remote electronic character of these chiral ligands can efficiently tuning the enantioselectivity by altering the length of the allylic C-Pd bond of the key catalytic intermediate.

Transition metal-catalyzed asymmetric synthesis is one of the most efficient methods for accessing chiral compounds, and it has found extensive applications in natural product synthesis, medicinal chemistry, and other areas[1–3]. The designing of efficient chiral ligands and the development of new reactions, which can enrich the toolbox of asymmetric synthesis, are core research areas in modern synthetic chemistry. By introducing steric hindrance groups into the coordination center to regulate the chiral ligand's steric environment[4,5], a primary strategy for catalyst design, chemists have achieved numerous highly efficient reactions. On the other hand, the remote electronic modulation under appropriate steric hindrance has been demonstrated to be another vital handle on catalyst design. In a seminal report in 1991, Jacobsen and co-workers unveiled a strong linear free energy relationship between the enantiomeric excess (ee) of epoxidation products and the electronic property of the *para*-substituents of (salen)-Mn catalysts, demonstrating that introducing strong electron-donating substituents could ensure excellent ee values (Fig. 1a)[6,7]. Thereafter, the importance of remote electronic effects in synthetic chemistry, such as asymmetric epoxidation, hydrofunctionalization of alkene, hydrogen bond-catalyzed reaction, site-selective acylation and others[8–13], has been increasingly appreciated. Nevertheless, the potential applications of remote electronic effect in Pd-catalyzed asymmetric transformations have remained largely unexplored[14,15], partly because the known effective chiral catalysts are not well-suited to remote electronic tuning either synthetically or structurally.

Among numerous privileged chiral ligands, 1,1′-binaphthol (BINOL)-derived phosphoramidites are one of the most widely used ligands in transition metal-catalyzed asymmetric reactions[16]. In addition to enabling the adjustment of the steric demand of the catalyst at the 3,3′-positions, the BINOL scaffold also provides us an opportunity to systematically turn the remote electronic feature by introducing

[1]Key Laboratory of Precision and Intelligent Chemistry and Department of Chemistry, University of Science and Technology of China, 230026 Hefei, P. R. China. [2]Key Laboratory of Green and Precise Synthetic Chemistry and Applications, Ministry of Education, Huaibei Normal University, 235000 Huaibei, P. R. China. [3]These authors contributed equally: Suchen Zou, Zeyu Zhao. e-mail: hanmin@ustc.edu.cn

https://doi.org/10.1038/s41467-024-54328-5

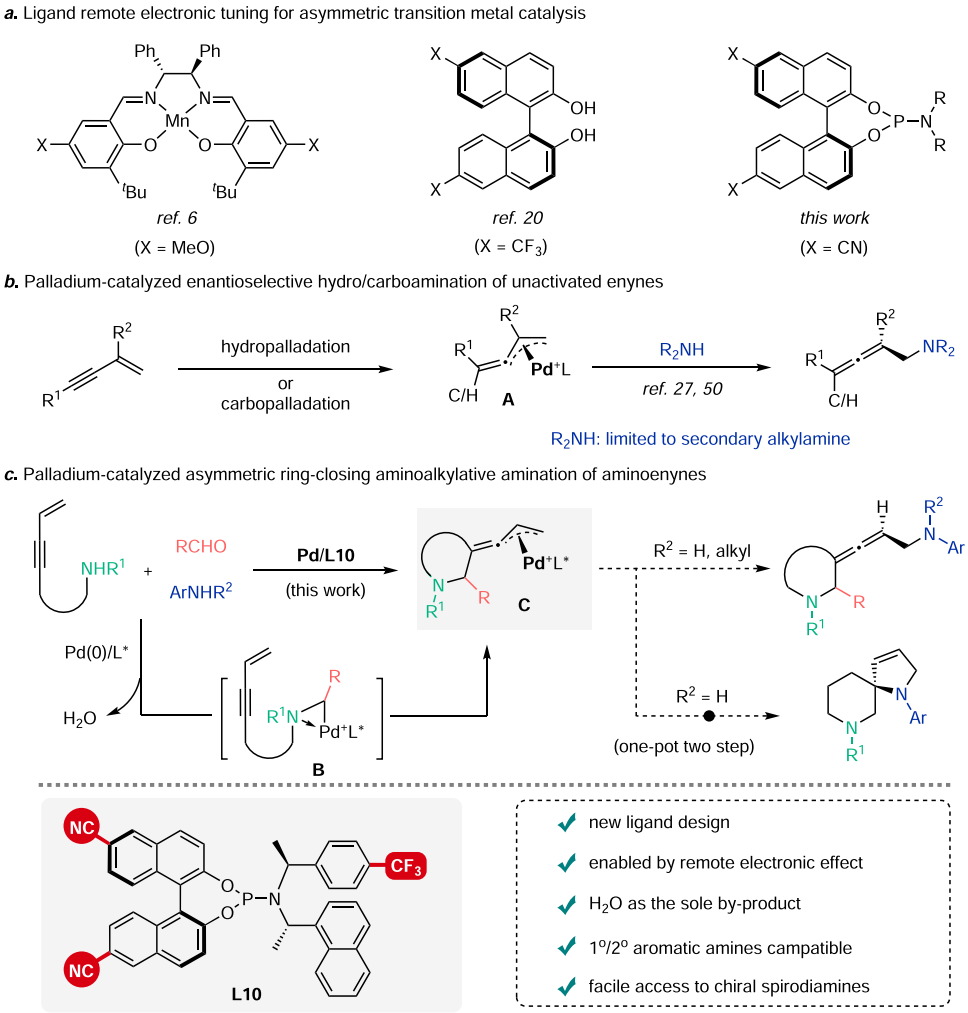

Fig. 1 | Pd-catalyzed enantioselective carboamination of unactivated enynes. **a** Ligand remote electronic tuning for asymmetric metal catalysis. **b** The current state-of-the-art of palladium-catalyzed asymmetric hydro/carboamination of enynes. **c** Tailored chiral phosphoramidite enables palladium-catalyzed asymmetric ring-closing aminoalkylative amination of aminoenynes.

different substituents at 6,6′-positions[17–19]. For instance, by introducing $-CF_3$ into the 6,6′-positions of BINOL, Kobayashi and co-workers achieved a highly enantioselective Mannich-type reaction of silyl enol ethers with aldimines, catalyzed by (6,6′-$(CF_3)_2$BINOL)-Zr, with a high level of TON (Fig. 1a)[20]. Despite these advances, most BINOL-derived phosphoramidites designed for Pd-catalyzed reactions relied on tuning the substituents at the 3,3′-positions of the BINOL-skeleton, rendering scant attention paid to achieving highly selective reactions by remote electronic tuning[5,16]. Hence, the investigation of the remote electronic effect in Pd-catalyzed asymmetric transformation by taking advantage of the BINOL-derived phosphoramidites holds great significance. In line with our continuous interest in designing chiral ligands[21,22] and developing asymmetric reactions based on aminoalkylation chemistry[23–27] herein, we report a Pd-catalyzed highly enantioselective ring-closing aminoalkylative amination of enynes, which was enabled by a remote −CN group decorated phosphoramidite ligand (Fig. 1).

Chiral allenes are an important class of molecules that not only exist in numerous natural and biologically important synthetic molecules[28] but also serve as useful building blocks for the efficient synthesis of diverse intricate molecules[29–31]. Specifically, densely functionalized 2,3-allenylamines are remarkably versatile due to the incorporation of two important transformable functional groups (allene and amine)[32–34], and they have found particularly elegant applications in the synthesis of natural products[35–37]. Accordingly, there are enduring endeavors to devise efficient methods for synthesizing these targets[38–49]. Of the many sophisticated catalytic methods, the Pd-catalyzed asymmetric two-component 1,4-hydro/carboamination of unactivated enynes constitutes the most atom- and step-economic routes for the rapid assembly of chiral allenylamines (Fig. 1b). However, relevant reports on this area remain scarce[27,50,51]. Furthermore, while the documented 1,4-functionalization of enynes can yield a range of enantioenriched allenylamines, they typically require the use of secondary alkylamines[50] or secondary alkylamine-derived aminals[27] to achieve acceptable enantioselectivities ((39–91% ee),[50] (67–93% ee)[27]). Aromatic amines, on the other hand, are omnipresent in natural products and bioactive compounds[52]. These compounds often exhibit enhanced stability, and their aryl groups can influence reactivity and selectivity in synthetic transformations. Expanding the nucleophiles from alkylamines to aromatic amines could further advance this field by enabling the synthesis of more complex and potentially bioactive molecules. However, extending these methods to the less nucleophilic aromatic amines remains a significant challenge.

Recently, we have disclosed a more atom-economic and environmentally benign three-component reaction towards racemic allenylamines[27], where the putative aminoalkyl cyclopalladated complex **B** was produced from the *N,O*-acetals that were generated in situ

via condensation of aminoenynes and aldehydes, with H_2O as the sole by-product (Fig. 1c). In light of the above-mentioned challenges and with this efficient three-component protocol in hand, we embarked on developing a more practical asymmetric variant to be compatible with aromatic amines. Mechanistically, the asymmetric allylic amination of allene acetates[46] and the asymmetric hydroamination of enynes,[50] which share the same vinyl η^3-allylic palladium **A**,[53] proceeded under the control of Curtin-Hammett principle with the amination of palladium-complex **A** being the stereo-determining step. As such, we surmised that the rationally designed chiral ligands, by fine-tuning their electronic properties, would potentially facilitate the desired carboamination with aromatic amines. If achievable, this protocol would offer an expedient approach to chiral exocyclic allenylamines bearing a saturated *N*-heterocycle (Fig. 1c). Moreover, primary aromatic amines may undergo a one-pot carboamination/hydroamination reaction, hopefully enabling the straightforward synthesis of chiral spirodiamines featured in many biologically active compounds[54]. These chiral spirocyclic structures are currently not easily accessible through other strategies[54–56].

Results

Preliminary results

Initially, the reaction of *N*-benzylhept-6-en-4-yn-1-amine **1a**, polyformaldehyde **2a**, and *N*-methylaniline **3a** was selected as the model system. The chiral ligand screening was performed in CH_2Cl_2 at −10 °C with 2.5 mol% of $[Pd(\pi\text{-cinnamyl})Cl]_2$ as catalyst precursor and 8 mol% of $AgClO_4$ as an additive. Employing the common chiral ligands utilized in Pd-catalyzed asymmetric reaction achieved limited success (for the details, see Supplementary Table 1). After many trials, it turned out that the reaction could proceed smoothly with phosphoramidite **L1**, previously reported in our previous work[27], as the chiral ligand and the target product **4** were obtained in 75% yield with 59% ee (Fig. 2a). To our delight, the chiral product **4** was obtained in 79% yield with 76% ee by lowering the reaction temperature to −30 °C.

Mechanistic investigations and reaction optimization

With these preliminary results in hand, we next sought to investigate the reaction mechanism, which may, in turn, guide the optimization of reaction conditions. The kinetic studies were carried out based on the initial reaction rate and demonstrated first-order dependence on the concentrations of the palladium catalyst, isolated *N,O*-acetal, and *N*-methyl aniline species (Fig. 2b). These results suggested that these three species were involved in the turnover-limiting step. Previous research has shown that electron-rich alkyl amines exhibit higher enantioselectivity compared to less nucleophilic aromatic amines[50]. This finding led us to hypothesize that the nucleophilicity of the nitrogen nucleophile could directly impact the stereoselectivity of the reaction. To this end, we used **1a** and formaldehyde **2a** as the standard substrates to react with a series of *N*-methyl anilines bearing different *para*-substituents under Pd/**L1** catalysis at −30 °C (Fig. 2c). The experimental results indicated that the ee value of the product increased with the increase of nucleophilicity of aromatic amine. Moreover, a linear free-energy relationship with good correlation ($R^2 = 0.95$) was observed in a plot of lg(er) against σ_p. The negative slope ($\rho = -0.69$) indicates that ee was highly sensitive to the nucleophilicity of the substrates. Collectively, these results suggest that the amination of vinyl η^3-allylpalladium complex **C** might be the turnover-limiting and stereo-determining step (Fig. 1c). In addition to these experiments, we investigated whether catalyst deactivation or product inhibition existed in this reaction. Firstly, we conducted a same-excess experiment (Fig. 2d, entries 1 and 2). Based on the first-order kinetic results from the initial rate experiments, we performed data fitting using variable time normalization analysis[57] (Figs. 2d-1, inset) and found that the plot fits well at lower conversions (around 20%). However, lower normalized rates were observed for lower catalyst loadings in the later stages of the reaction, suggesting potential product inhibition or catalyst deactivation. An additional control experiment with the product as an additive was performed (Fig. 2d, entries 1 and 3). The results showed that adding 25% of the product led to a decrease in the initial reaction rate (Fig. 2d-2), indicating that the reaction suffers from product inhibition. This inhibition may be caused by the coordination of the allene to the low-valent palladium species[58] (for the proposed reaction mechanism, see Supplementary Fig 21). Therefore, it is also important to ensure that the catalyst remains active throughout the reaction during the optimization process.

Encouraged by these results, we envisioned that improving the electrophilicity of vinyl η^3-allylic palladium intermediate by minimizing the electron-donating ability of ligands could improve the catalytic efficiency and lead to higher enantioselectivity. Modification of the phosphoramidite ligand **L1** was then conducted to improve the performance of the asymmetric catalytic system. As shown in Fig. 3a, variation of the chiral amine unit of the ligand **L1** revealed that the more electron-rich the ligand used, the lower the enantioselectivity of the products was observed, whereas the yield remained unaffected (Fig. 3a, **L1**–**L4**). Inspired by these and our previous results[27] that the introduction of substituents at the 3,3′-position of the chiral BINOL-framework resulted in a significant decrease in reaction efficiency, we turned to modify the ligand **L1** with different substituents at the 6,6′-position of the BINOL-skeleton. This allows for tuning the remote electronic properties of the ligand without altering its steric hindrance. Along this line, five new phosphoramidite ligands (**L5**–**L9**) with different substituents, including $-^t$Bu, −Cl, −Br, $-CO_2Me$, and $-CF_3$ were successfully prepared. The structure of ligand **L6** was characterized by X-ray crystallography analysis. As expected, the ee value of the product gradually increased along with the decrease of the electron-donation ability of the ligand (Fig. 3a, **L5**–**L9**), and 91% ee was obtained with **L9** as the ligand. Bolstered by these promising results, we next synthesized a more electron-deficient ligand **L10** bearing−CN substituent at the 6,6′-position of the BINOL-skeleton and investigated its catalytic performance. As expected, the corresponding product **4** was obtained in good yield (78%) with excellent ee value (97%). Further screening of other parameters with **L10** as the ligand indicates that the current reaction conditions are optimal (for details, see Supplementary Tables 8 and 9).

Investigations on ligand electronic effect

During the above ligand screening process, we observed an intriguing relationship between the enantioselectivity of product **4** and the σ_p parameter of the substituents at the C-6 position of the ligand (Fig. 3b)[59]. A linear free-energy relationship with good correlation ($R^2 = 0.92$) was observed in a plot of lg(er) against σ_p. The positive slope ($\rho = 1.35$) indicated that the ee was highly sensitive to the remote electronic nature of the ligand used here. To probe the electronic effect and to deeply understand the behavior of **L10** in controlling the enantioselectivity, a series of experiments were conducted. A non-linear effect experiment was conducted and showed a linear relationship, indicating that the palladium-to-ligand ratio in the stereo-determining step is most likely 1:1 (Fig. 3c). The reaction rates were compared using different ligands at room temperature. As shown in Fig. 3d, reactions with ligands bearing electron-withdrawing groups exhibited a faster rate compared to those with electron-donating groups, with the reaction rate order as follows: **L10** > **L6** > **L5**. According to previous reports[60,61], electron-deficient ligands facilitate the reductive elimination step from higher oxidation state metals to lower oxidation states. Thus, by combining the results from the non-linear effect experiments and kinetics results, we tentatively conclude that the allylic substitution process from Pd(II) to Pd(0) is most likely to be the turnover-limiting step, with only monomeric palladium catalysts involved in this process. DOSY NMR of the cationic Pd/**L10** complex revealed that a single complex forms when palladium and the

https://doi.org/10.1038/s41467-024-54328-5

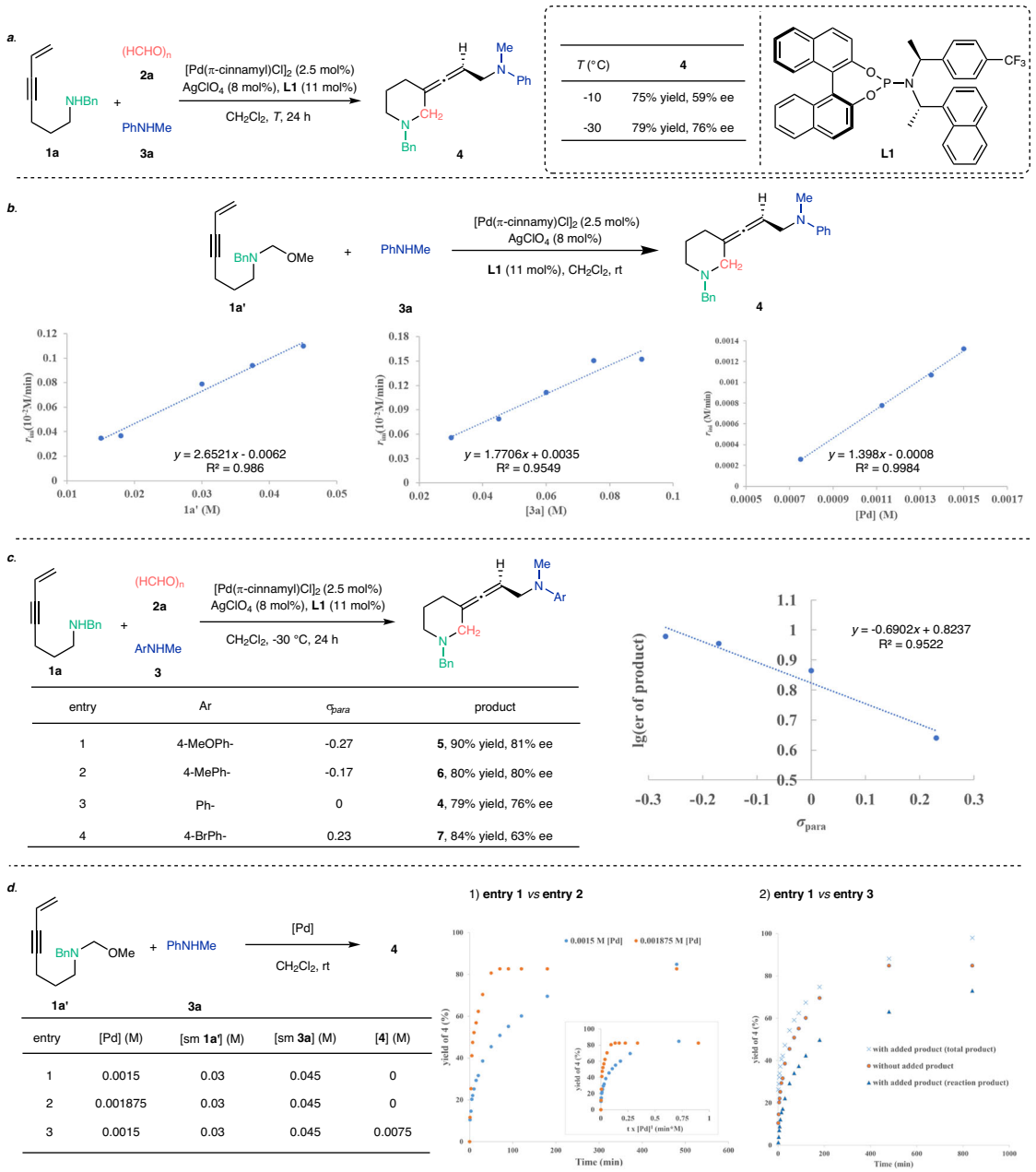

Fig. 2 | Preliminary results and mechanistic investigations. a Preliminary results with phosphoramidite **L1** as the ligand. **b** Kinetic analysis. **c** Hammett plot for the enantiomeric ratio of products using *para*-substituted anilines. **d** Experiments designed to identify the potential product inhibition or catalyst deactivation.

ligand are combined in a 1:1 ratio, with no oligomeric allyl species detected, which might further support our hypothesis (for details, see Supplementary Table 12). During the optimization of the reaction conditions, we observed that varying the ratio of Pd/**L10** from 1:2 to 1:1 had no influence on the enantioselectivities of this reaction, but it conspicuously attenuated the reactivity (for details, see Supplementary Table 8). Given the presence of catalyst deactivation and product inhibition in this reaction (Fig. 2d), this result suggests that an appropriate excess of ligand would mitigate catalyst deactivation[62]. Additionally, we performed DFT calculations to investigate the effect of substituents on the electron density of the palladium center. The results indicated that, in the allylic cationic palladium complex, the electron density at the palladium center is directly influenced by the remote substituents of the ligand, with electron-withdrawing groups rendering the palladium center more electron-deficient (for details, see Supplementary Table 13). Accordingly, we assumed that the η^3-allylic moiety of the complex would be closer to the more electron-deficient palladium center, which thus enhances its electrophilicity to facilitate the desired reaction. To validate this hypothesis, three new palladium–phosphoramidite complexes, Pd(allyl)**L5**Cl (**Pd-1**), Pd(allyl)**L6**Cl (**Pd-2**) and Pd(allyl)**L10**Cl (**Pd-3**) were prepared and characterized by X-ray crystallography analysis (Fig. 3e). The X-ray structures of [Pd(allyl)**L***Cl] illustrated the order of bond lengths of allylic-C-Pd at the *trans*-position of P-Pd as follows: **Pd-1** (2.203 Å) > **Pd-2** (2.187 Å) > **Pd-3** (2.177 Å). These results confirmed that reducing the electron-donating ability of ligands could increase the electrophilicity of vinyl η^3-allylic palladium species, thereby increasing the reaction rate. Moreover, the allyl group closer to the palladium center can amplify the discriminating interaction between the diastereotopic vinyl η^3-allylic palladium complex and amine, thus improving the kinetic selectivity at the amination step and resulting in higher levels of enantioselectivity.

https://doi.org/10.1038/s41467-024-54328-5

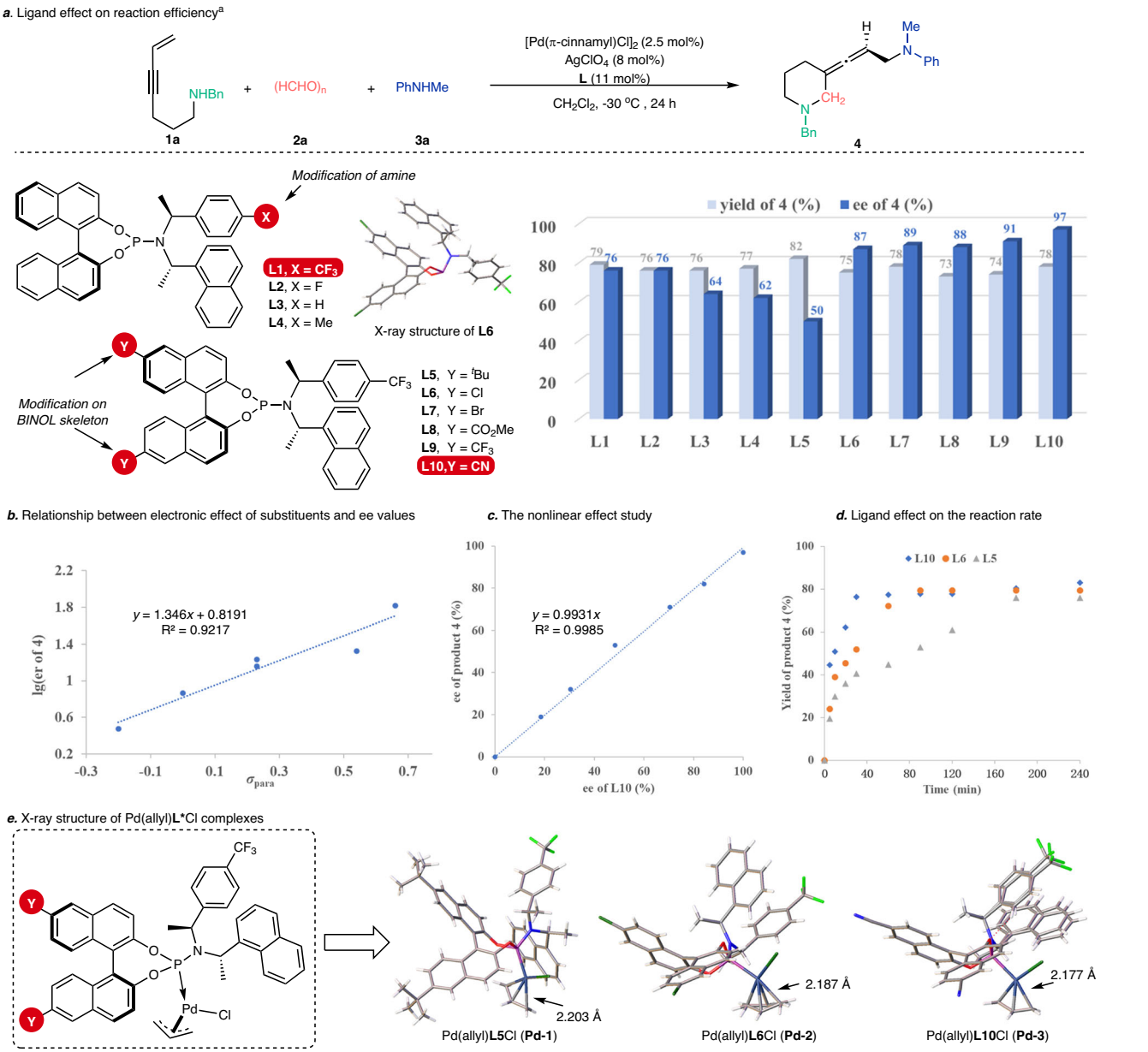

Fig. 3 | Modification and effect of ligands. a Ligand effect on reaction efficiency. **b** Relationship between the remote electronic effect of substituents and ee values. **c** The nonlinear effect study. **d** Ligand effect on the reaction rate. **e** X-ray structure of Pd(allyl)**L***Cl complexes. [a]Conditions: **1a** (0.3 mmol), **2a** (0.45 mmol), **3a** (0.45 mmol), [Pd(π-cinnamyl)Cl]$_2$ (2.5 mol%), $AgClO_4$ (8 mol%), **L** (11 mol%), CH_2Cl_2 (1.5 mL), −30 °C, 24 h, isolated yield.

Substrate scope exploration

With this catalytic system in hand, we set out to investigate the substrate generality of this Pd-catalyzed three-component ring-closing reaction. First, the influence of various substituents on the phenyl group of *N*-methyl anilines was explored (Fig. 4A). To our delight, both electron-withdrawing group (−Cl, −Br, −CO_2Me) and -donating groups (−OMe, −Me) were all compatible with this reaction and afforded the desired products (**4**-**12**) in 65–85% yields with 75–99% ee values. Notably, with the catalyst loading reduced to 1 mol%, the desired product **4** could still be obtained in 67% isolated yield with 94% ee, demonstrating the robustness and efficiency of this protocol. Moreover, the electronic nature of the phenyl ring of the *N*-methylanilines had a strong influence on the enantioselectivities. The *N*-methylanilines bearing mono-halide furnished the corresponding chiral allenes (**7** and **8**) in good yields with excellent ee. However, the reaction with strong electron-withdrawing group substituted *N*-methylanilines, such as ester or di-chlorine substituted substrates, provided lower enantioselectivities, while the yield remained unaffected (**10** and **11**). Compared with the results of the substrates bearing an electron-withdrawing group, the presence of an electron-donating group led to good yields with excellent enantioselectivities (**5**, **6**, **9**, and **12**). Furthermore, *N*-methyl naphthylamine showed good compatibility to produce the corresponding product **13** in 74% yield with 96% ee. In addition to *N*-methylanilines, other *N*-substituted anilines, such as ethyl, benzyl, allyl, and siloxane are amenable to this reaction, delivering the target product (**14**-**17**) with high to excellent ee values. For aniline tethered with a cyano group, a good yield was obtained (**18**) but with a lower ee value, which might be ascribed to its increased steric hindrance and potential coordination ability with the catalyst. Delightfully, 1,2,3,4-tetrahydroquinoline underwent the reaction efficiently, affording the target product **19** in 73% yield with 98% ee. The *N*-Ts-protected arylamine was also compatible with this transformation, affording the corresponding product **20** in 50% yield with excellent enantioselectivity (95% ee). However, an elevated temperature was

https://doi.org/10.1038/s41467-024-54328-5

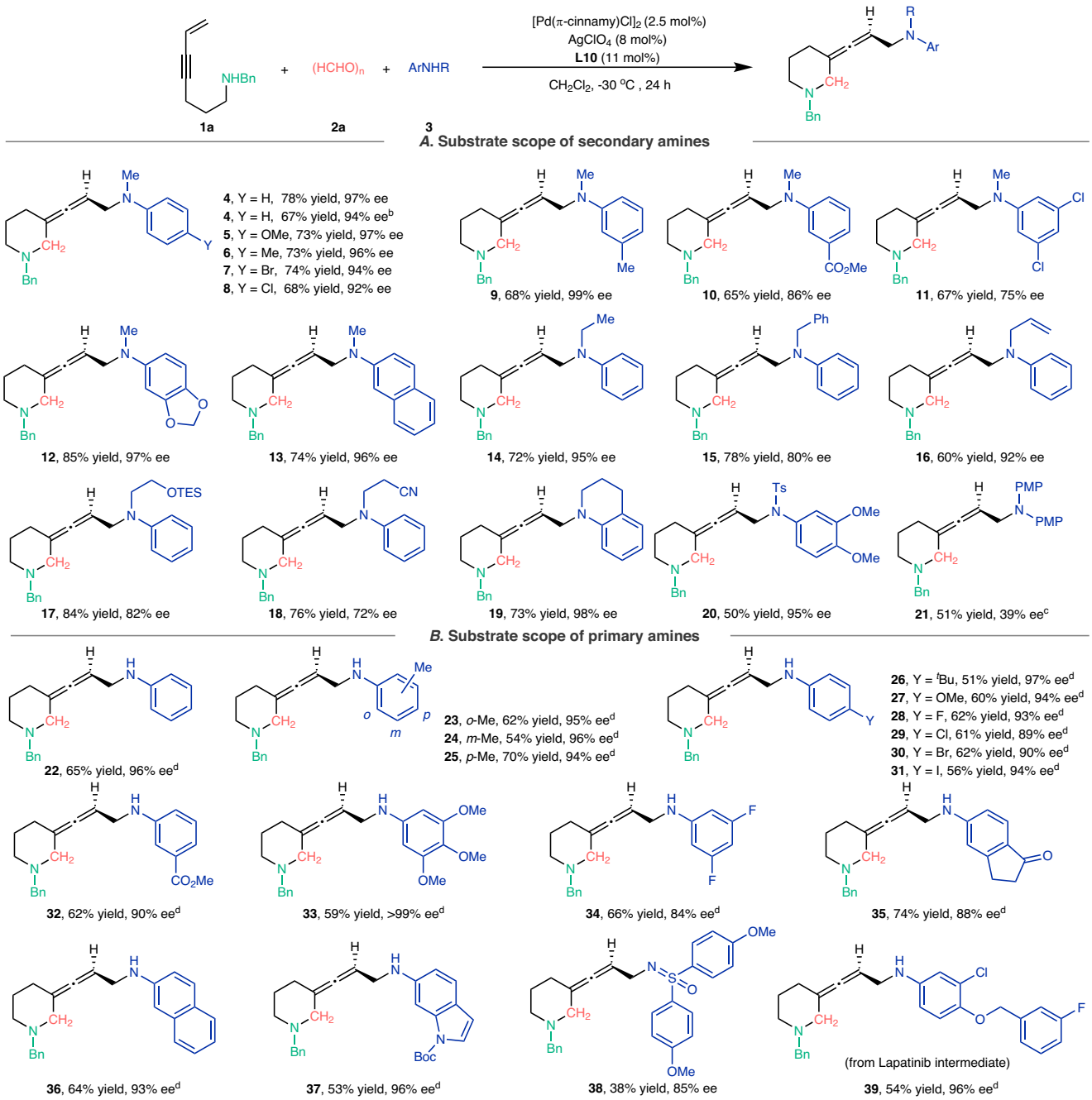

Fig. 4 | Substrate scope of amines. [a]Conditions: **1a** (0.3 mmol), **2a** (0.45 mmol), **3** (0.45 mmol), [Pd(π-cinnamyl)Cl]$_2$ (2.5 mol%), $AgClO_4$ (8 mol%), **L10** (11 mol%), CH_2Cl_2 (1.5 mL), −30 °C, 24 h, isolated yield. [b][Pd(π-cinnamyl)Cl]$_2$ (0.5 mol%), $AgClO_4$ (8 mol%), **L10** (2.2 mol%). [c]40 °C. [d]**1a** (0.3 mmol), **2a** (0.45 mmol), **3** (0.6 mmol), $Pd(CH_3CN)_2Cl_2$ (5 mol%), $AgClO_4$ (30 mol%), **L10** (11 mol%), CH_2Cl_2 (1.5 mL), −10 °C, 20 h, isolated yield. Ts *p*-toluenesulfonyl, PMP *p*-methoxyphenyl, Boc *t*-butyloxy carbonyl.

required for diarylamine to obtain the desired product, but the enantioselectivity was lower (**21**). Compared to our previous reaction system[27], this catalytic system can convert secondary alkylamine-derived aminals to the corresponding product with better ee under milder conditions but with a lower yield (for details, see Supplementary Fig 34).

Apart from secondary amines, primary arylamines are also competent. Only minor adjustments to the reaction conditions were needed to achieve the efficient cross-coupling with aniline, delivering the corresponding allene **22** in 65% yield with 96% ee (Fig. 4B). Similar to the reaction with secondary anilines, substrates bearing either electron-donating groups or electron-withdrawing groups on the phenyl ring all proceeded in high enantioselectivities (84–>99% ee) and moderate to good yields (51–74%). In particular, the reaction could tolerate sensitive functional groups, including Br (**30**) and I (**31**), which are useful features for further synthetic transformations. Moreover, naphthylamine and 6-azaindole were also suitable for delivering the corresponding products (**36** and **37**). Most intriguingly, diaryl sulfoximine, as an excellent ammonia surrogate and also an important pharmacophore in its own right[63] was compatible with this catalytic process, converting to corresponding product **38** in acceptable yield with good ee. Unfortunately, no desired products were detected when other amine sources, such as $TsNH_2$, $BocNH_2$, Boc_2NH, and $BnNH_2$, were subjected to the reaction. Encouraged by the good functional

https://doi.org/10.1038/s41467-024-54328-5

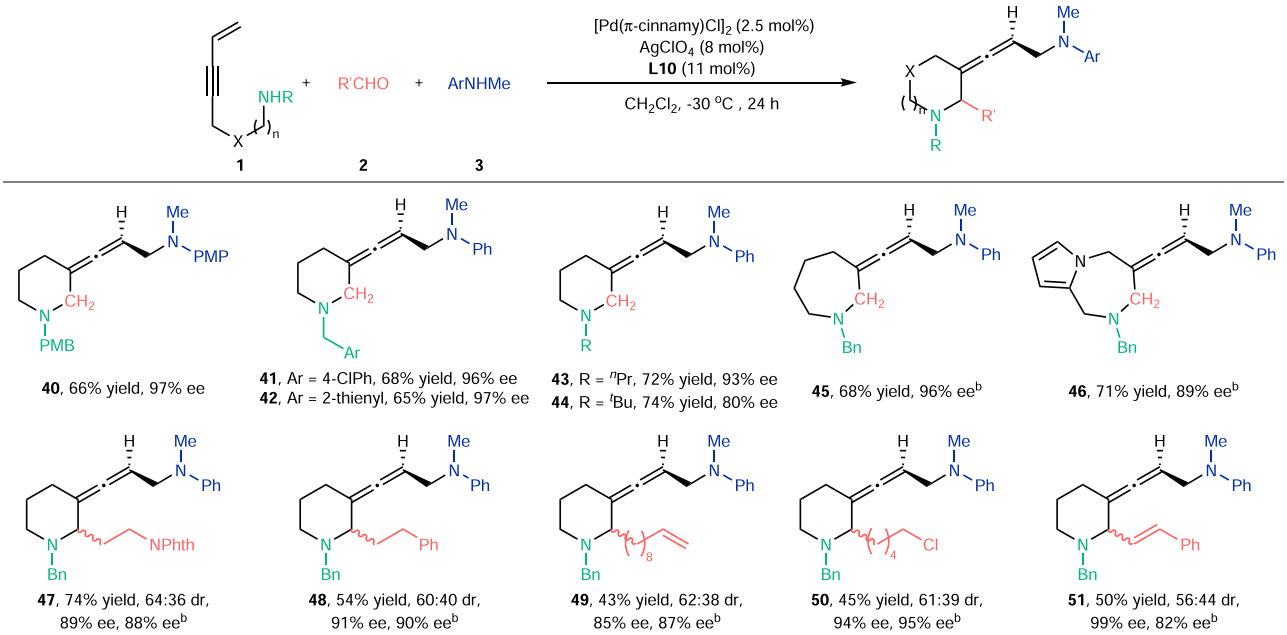

Fig. 5 | Substrate scope of aminoenynes and aldehydes. [a]Conditions: **1** (0.3 mmol), **2** (0.45 mmol), **3** (0.45 mmol), [Pd(π-cinnamyl)Cl]$_2$ (2.5 mol%), $AgClO_4$ (8 mol%), **L10** (11 mol%), CH_2Cl_2 (1.5 mL), −30 °C, 24 h, isolated yield. [b]−30 °C, 36 h. PMP *p*-methoxyphenyl, PMB *p*-methoxybenzyl, NPhth phthalimide.

group compatibility of this reaction, we subsequently assessed its applicability to a biologically active compound. As shown in Fig. 4B, Lapatinib intermediate was subjected to this protocol, delivering the target product **39** in 54% yield with 96% ee.

We next turned our attention to investigating the substrate scope of aminoenynes and aldehydes. As demonstrated in Fig. 5, a variety of hept-6-en-4-yn-1-amines with different substituents on the nitrogen atom reacted smoothly to furnish the corresponding products (**40-44**) in 65–74% yields with excellent enantioselectivities (80–97% ee). Extending the tether length provided the exocyclic chiral allenylamines bearing a 7-membered ring in good yields with excellent ee values (**45** and **46**). However, no target product was detected when introducing substituents into the alkene group of aminoenynes. In addition to polyformaldehyde, we also investigated the compatibility of substituted aldehydes. To our delight, this three-component one-pot reaction was amenable to a wide range of aliphatic aldehydes bearing phthalimide, phenyl, alkenyl, and chlorine functional groups, affording the chiral exocyclic allenes (**47-50**) in moderate yields with high ee values, albeit with low diastereoselectivities. Moreover, α,β-unsaturated aldehyde also underwent the reaction smoothly (**51**). However, the current reaction conditions fail to convert aromatic aldehydes into the corresponding products, which might be attributed to the difficulty in forming the key aminoalkyl cyclopalladated complex **B** due to the large steric hindrance of the aryl group.

Construction of chiral spirodiamines

Over the last decades, there has been a growing recognition of spirocyclic scaffolds as promising building blocks in medicinal chemistry[64]. Moreover, recent research has demonstrated that replacing traditional flat aromatic cores of drug candidates with sp^3-rich templates can be highly beneficial.[65] In this respect, spirocyclic scaffolds bearing saturated *N*-heterocycles and a chiral spiro quaternary carbon are particularly attractive[54,66–68]. However, despite great efforts in this area, the catalytic enantioselective synthesis of this type of skeleton is still a daunting challenge. As shown in Fig. 6, with primary amines as the reaction partners, we can handily get the chiral spirodiamines through subsequent axial-to-center transfer by treating the reaction mixture with the catalytic amount $AgNO_3$. A series of arylamines were successfully employed in our process by using the tailored phosphoramidite ligand **L10**, providing chiral spirodiamines **52**–**58** in moderate yields along with good to excellent ee values (85–97% ee). Notably, the introduction of 6-azaindole could be accomplished and the chiral product **59** was obtained smoothly with high enantioselectivity. Finally, the structure of chiral spirodiamine **59** was unambiguously confirmed by X-ray analysis.

Synthetic transformations

The efficiency and practicality of the reaction were further demonstrated by the large-scale experiments and functional group transformations. As shown in Fig. 7a, under the standard reaction conditions, products **4** and **22** were smoothly obtained on a gram scale (0.89 and 0.66 g, respectively) in good yields with excellent ee values. Several transformations of chiral allene **22** were carried out (Fig. 7b). Treatment of **22** with 2.2 equivalents of NBS yielded dibrominated spirocyclic product **60** in 79% yield with 92% ee. When **22** was mixed with NIS at 0 °C for 12 h, the iodinated spiro-product **61** was formed in 77% yield with 90% ee. Through a Pd-catalyzed arylamination of allene, a phenyl group could be introduced into product **22** to produce product **62** in high yield with excellent enantioselectivity. Moreover, treating **22** with benzoyl chloride afforded the corresponding amide **63** in 91% yield. Furthermore, product **22** can be easily converted to spirodiamine **52** in good yield with a slight loss of enantiopurity under $AgNO_3$ catalysis. Selective hydrogenation of the double bond of **52** under PtO_2 catalysis in a hydrogen atmosphere afforded compound **64** in nearly quantitative yield. Additionally, the benzyl group in compound **52** could be readily removed using 1-chloroethyl chloroformate, and the resulting secondary amine could be transformed into sulfonamide **65** through subsequent sulfonation in 73% overall yield.

Discussion

In summary, we have demonstrated that the manipulation of electronic properties of remote substituents on BINOL-derived phosphoramidite ligands enables the optimization of Pd-catalyzed asymmetric ring-closing carboamination of enynes. With a tailored electron-deficient chiral phosphoramidite ligand, a broad range of aromatic amines can be compatible with this reaction, yielding a variety of enantiomerically enriched exocyclic allenylamines bearing saturated

https://doi.org/10.1038/s41467-024-54328-5

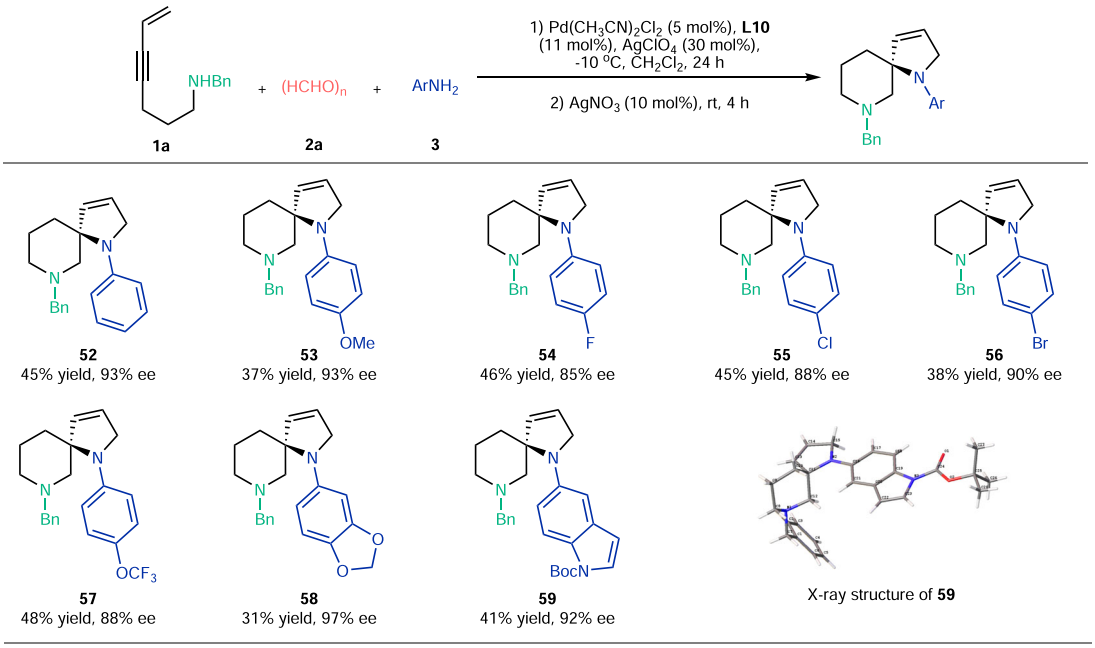

Fig. 6 | Access to chiral spirodiamines. Conditions: (1) **1a** (0.3 mmol), **2a** (0.45 mmol), **3** (0.6 mmol), $Pd(CH_3CN)_2Cl_2$ (5 mol%), $AgClO_4$ (30 mol%), **L10** (11 mol%), CH_2Cl_2 (1.5 mL), −10 °C, 24 h. (2) $AgNO_3$ (10 mol%), rt, 4 h, isolated yield. Boc *t*-butyloxy carbonyl.

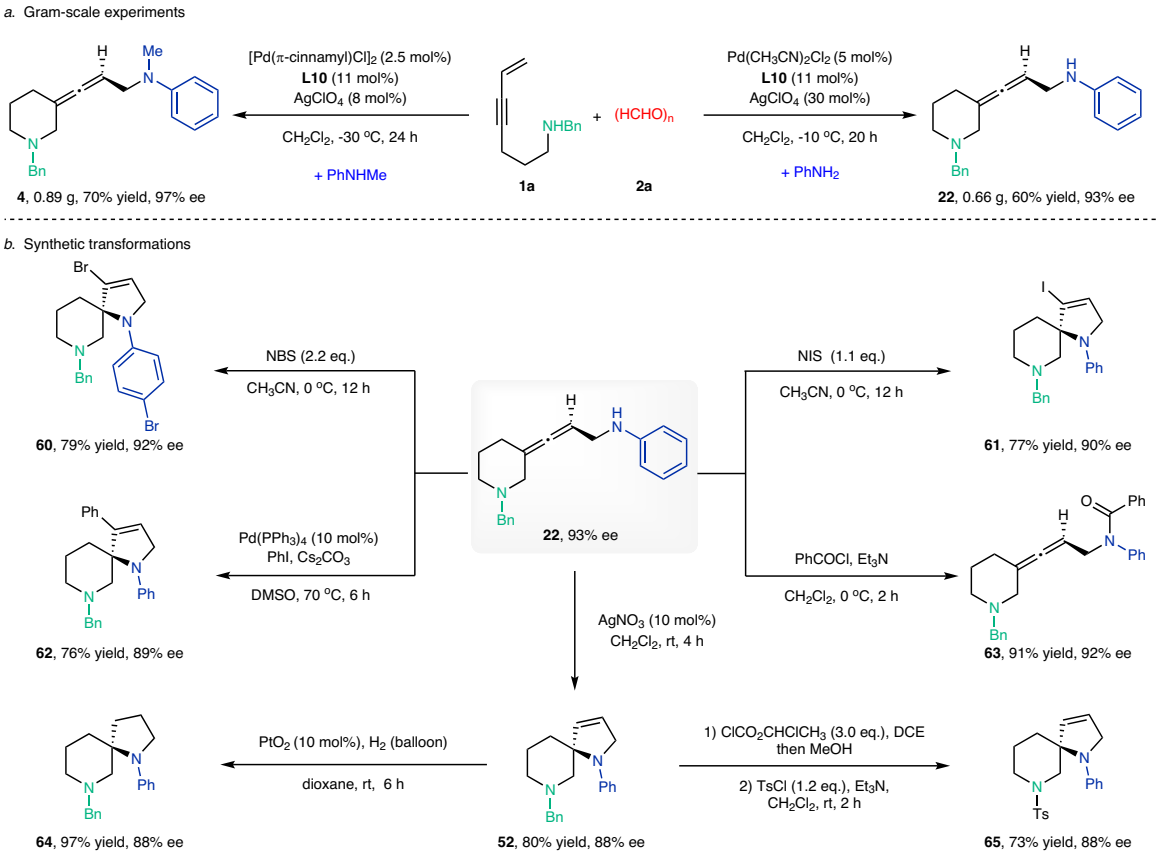

Fig. 7 | Gram-scale experiments and synthetic transformations. a Gram-scale experiments. **b** Synthetic transformations. NBS *N*-bromosuccinimide, NIS *N*-iodosuccinimide, Ts *p*-toluenesulfonyl.

N-heterocycles. Additionally, employing this catalytic system, a one-pot axial-to-central chirality transfer process was devised, which enables the expedient construction of valuable chiral spirodiamines. The robustness and efficiency of our approach should hold potential for applications in complex molecule synthesis and drug discovery. More broadly, we anticipate that this study may inspire further exploration of remote electronic effects of chiral ligands to address other untapped catalytic asymmetric reactions.

Methods

General procedure for the asymmetric reactions of aminoenynes, paraformaldehyde and secondary amines

Step 1. To a Young-type tube equipped with a magnetic stirrer was added **1** (0.3 mmol), paraformaldehyde **2a** (10.8 mg, 0.45 mmol), K_2CO_3 (8.3 mg, 20 mol%), anhydrous Na_2SO_4 (8.5 mg, 20 mol%) and MeOH (1.0 mL). The reaction mixture was stirred at 40 °C for 2 h. After evaporation of the solvent under reduced pressure, CH_2Cl_2 (1.0 mL) was added under the N_2 atmosphere and used directly for the next step.

Step 2. In an N_2-filled glove box, $[Pd(\pi\text{-cinnamyl})Cl]_2$ (3.9 mg, 2.5 mol%), $AgClO_4$ (5.0 mg, 8 mol%), **L10** (23.3 mg, 11 mol%) and CH_2Cl_2 (0.5 mL) were added to a flame-dried Young-type tube (25 mL). The mixture was stirred at room temperature for 30 min. After that, **3** (0.45 mmol) and the crude product of *Step 1* in CH_2Cl_2 were added to the mixture under the N_2 atmosphere. The reaction mixture was degassed with freeze–thaw method for one time and stirred at −30 °C for 24 h. After evaporation of the solvent under reduced pressure, the residue was purified by flash column chromatography on silica gel to give the desired product. The ee value was determined by HPLC analysis with the chiral column.

General procedure for the asymmetric reactions of aminoenynes, paraformaldehyde, and primary amines

Step 1. To a Young-type tube equipped with a magnetic stirrer was added **1** (0.3 mmol), paraformaldehyde **2a** (10.8 mg, 0.45 mmol), K_2CO_3 (8.3 mg, 20 mol%), anhydrous Na_2SO_4 (8.5 mg, 20 mol%), and MeOH (1.0 mL). The reaction mixture was stirred at 40 °C for 2 h. After evaporation of the solvent under reduced pressure, CH_2Cl_2 (1.0 mL) was added under the N_2 atmosphere and used directly for the next step.

Step 2. In an N_2-filled glove box, $Pd(CH_3CN)_2Cl_2$ (3.9 mg, 5 mol%), $AgClO_4$ (18.6 mg, 30 mol%), **L10** (23.3 mg, 11 mol%), and CH_2Cl_2 (0.5 mL) were added to a flame-dried Young-type tube (25 mL). The mixture was stirred at 40 °C for 30 min. After cooling to room temperature, **3** (0.6 mmol) and the crude product of *Step 1* in CH_2Cl_2 were added to the mixture under an N_2 atmosphere. The reaction mixture was degassed with freeze–thaw method for one time and stirred at −10 °C for 20 h. After evaporation of the solvent under reduced pressure, the residue was purified by flash column chromatography on silica gel to give the desired product. The ee value was determined by HPLC analysis with the chiral column.

General procedure for the asymmetric reactions of aminoenynes, substituted aldehyde and amines

In an N_2-filled glove box, $[Pd(\pi\text{-cinnamyl})Cl]_2$ (3.9 mg, 2.5 mol%), $AgClO_4$ (5.0 mg, 8 mol%), **L10** (23.3 mg, 11 mol%) and CH_2Cl_2 (1.5 mL) were added to a flame-dried Young-type tube (25 mL). The mixture was stirred at room temperature for 30 min. After that, **1** (0.3 mmol), aldehyde **2** (0.45 mmol), and **3** (0.45 mmol) were added to the mixture under N_2 atmosphere. The reaction mixture was degassed with freeze-thaw method for one time and stirred at −30 °C for 36 h. After evaporation of the solvent under reduced pressure, the residue was purified by flash column chromatography on silica gel to give the desired product. The ee value was determined by HPLC analysis with the chiral column.

General procedure to access chiral spirodiamines

Step 1. To a Young-type tube equipped with a magnetic stirrer was added **1** (0.3 mmol), paraformaldehyde **2a** (10.8 mg, 0.45 mmol), K_2CO_3 (8.3 mg, 20 mol%), anhydrous Na_2SO_4 (8.5 mg, 20 mol%) and MeOH (1.0 mL). The reaction mixture was stirred at 40 °C for 2 h. After evaporation of the solvent under reduced pressure, CH_2Cl_2 (1.0 mL) was added under N_2 atmosphere and used directly for next step.

Step 2. In an N_2-filled glove box, $Pd(CH_3CN)_2Cl_2$ (3.9 mg, 5 mol%), $AgClO_4$ (18.6 mg, 30 mol%), **L10** (23.3 mg, 11 mol%), and CH_2Cl_2 (0.5 mL) were added to a flame-dried Young-type tube (25 mL). The mixture was stirred at 40 °C for 30 min. After cooling to room temperature, **3** (0.6 mmol) and the crude product of *Step 1* in CH_2Cl_2 were added to the mixture under an N_2 atmosphere. The reaction mixture was degassed with freeze–thaw method for one time and stirred at −10 °C for 24 h.

Step 3. To the above reaction mixture was added $AgNO_3$ (5.1 mg, 10 mol%), then stirred at rt for 4 h. After evaporation of the solvent under reduced pressure, the residue was purified by flash column chromatography on silica gel to give the desired product. The ee value was determined by HPLC analysis with chiral column.

Data availability

All data supporting the findings of this study are available within the article and its Supplementary Information files or from the corresponding author upon request. Crystallographic data for the structures reported in this article have been deposited at the Cambridge Crystallographic Data Centre, under deposition numbers CCDC 2262824 (**L6**), 2335182 (**Pd-1**), 2335183 (**Pd-2**), 2335184 (**Pd-3**), and 2335185 (**59**). Copies of the data can be obtained free of charge via https://www.ccdc.cam.ac.uk/structures/. Source data are provided with this paper.

References

1. Li, C., Ragab, S. S., Liu, G. & Tang, W. Enantioselective formation of quaternary carbon stereo-centers in natural product synthesis: a recent update. *Nat. Prod. Rep.* **37**, 276–292 (2020).
2. Mei, G.-J., Koay, W. L., Tan, C. X. A. & Lu, Y. Catalytic asymmetric preparation of pyrroloindolines: strategies and applications to total synthesis. *Chem. Soc. Rev.* **50**, 5985–6012 (2021).
3. Yang, H., Yu, H., Stolarzewicz, I. A. & Tang, W. Enantioselective transformations in the synthesis of therapeutic agents. *Chem. Rev.* **123**, 9397–9446 (2023).
4. Mas-Roselló, J., Herraiz, A. G., Audic, B., Laverny, A. & Cramer, N. Chiral cyclopentadienyl ligands: design, syntheses, and applications in asymmetric catalysis. *Angew. Chem. Int. Ed.* **60**, 13198–13224 (2021).
5. Fu, W. & Tang, W. Chiral monophosphorus ligands for asymmetric catalytic reactions. *ACS Catal.* **6**, 4814–4858 (2016).
6. Jacobsen, E. N., Zhang, W. & Güler, M. L. Electronic tuning of asymmetric catalysts. *J. Am. Chem. Soc.* **113**, 6703–6704 (1991).
7. Palucki, M. et al. The mechanistic basis for electronic effects on enantioselectivity in the (salen)Mn(III)-catalyzed epoxidation reaction. *J. Am. Chem. Soc.* **120**, 948–954 (1998).
8. Flanagan, S. P. & Guiry, P. J. Substituent electronic effects in chiral ligands for asymmetric catalysis. *J. Organomet. Chem.* **691**, 2125–2154 (2006).
9. Casalnuovo, A. L., RajanBabu, T. V., Ayers, T. A. & Warren, T. H. Ligand electronic effects in asymmetric catalysis: enhanced enantioselectivity in the asymmetric hydrocyanation of vinylarenes. *J. Am. Chem. Soc.* **116**, 9869–9882 (1994).
10. Yang, D., Yip, Y.-C., Chen, J. & Cheung, K.-K. Significant effects of nonconjugated remote substituents in catalytic asymmetric epoxidation. *J. Am. Chem. Soc.* **120**, 7659–7660 (1998).
11. Jensen, K. H. & Sigman, M. S. Evaluation of catalyst acidity and substrate electronic effects in a hydrogen bond-catalyzed enantioselective reaction. *J. Org. Chem.* **75**, 7194–7201 (2010).
12. Ho, C.-Y., Chan, C.-W. & He, L. Catalytic asymmetric hydroalkenylation of vinylarenes: electronic effects of substrates and chiral N-heterocyclic carbene ligands. *Angew. Chem. Int. Ed.* **54**, 4512–4516 (2015).
13. Wilcock, B. C. et al. Electronic tuning of site-selectivity. *Nat. Chem.* **4**, 996–1003 (2012).

14. Tu, T., Hou, X.-L. & Dai, L.-X. Ligand electronic effects in the palladium-catalyzed asymmetric allylic alkylation reaction with planar chiral diphosphine-oxazoline ferrocenyl ligands. *J. Organomet. Chem.* **689**, 3847–3852 (2004).
15. Jensen, K. H., Webb, J. D. & Sigman, M. S. Advancing the mechanistic understanding of an enantioselective palladium-catalyzed alkene difunctionalization reaction. *J. Am. Chem. Soc.* **132**, 17471–17478 (2010).
16. Teichert, J. F. & Feringa, B. L. Phosphoramidites: privileged ligands in asymmetric catalysis. *Angew. Chem. Int. Ed.* **49**, 2486–2528 (2010).
17. Pu, L. Regioselective substitution of BINOL. *Chem. Rev.* **124**, 6643–6689 (2024).
18. Vallavoju, N., Selvakumar, S., Jockusch, S., Sibi, M. P. & Sivaguru, J. Enantioselective organo-photocatalysis mediated by atropisomeric thiourea derivatives. *Angew. Chem. Int. Ed.* **53**, 5604–5608 (2014).
19. Yan, S.-Y. et al. Palladium(II)-catalyzed enantioselective arylation of unbiased methylene C(sp^3)–H bonds enabled by a 2-pyridinylisopropyl auxiliary and chiral phosphoric acids. *Angew. Chem. Int. Ed.* **57**, 9093–9097 (2018).
20. Ishitani, H., Ueno, M. & Kobayashi, S. Enantioselective Mannich-type reactions using a novel chiral zirconium catalyst for the synthesis of optically active *β*-amino acid derivatives. *J. Am. Chem. Soc.* **122**, 8180–8186 (2000).
21. Shi, D., Xie, Y., Zhou, H., Xia, C. & Huang, H. A highly diastereo- and enantioselective reaction for constructing functionalized cyclohexanes: six contiguous stereocenters in one step. *Angew. Chem. Int. Ed.* **51**, 1248–1251 (2012).
22. Chen, X., Gao, B., Su, Y. & Huang, H. Enantioselective epoxidation of electron-deficient alkenes catalyzed by manganese complexes with chiral N_4 ligands derived from rigid chiral diamines. *Adv. Synth. Catal.* **359**, 2535–2541 (2017).
23. Zhang, H., Jiang, T., Zhang, J. & Huang, H. Catalytic reactions directed by a structurally well-defined aminomethyl cyclopalladated complex. *Acc. Chem. Res.* **54**, 4305–4318 (2021).
24. Liu, Y., Xie, Y., Wang, H. & Huang, H. Enantioselective aminomethylamination of conjugated dienes with aminals enabled by chiral palladium complex-catalyzed C–N bond activation. *J. Am. Chem. Soc.* **138**, 4314–4317 (2016).
25. Chang, R., Cai, S., Yang, G., Yan, X. & Huang, H. Asymmetric aminomethylative etherification of conjugated dienes with aliphatic alcohols facilitated by hydrogen bonding. *J. Am. Chem. Soc.* **143**, 12467–12472 (2021).
26. Zou, S., Yu, B. & Huang, H. Enantioselective ring-closing aminomethylamination of aminodienes enabled by modified Trost ligands. *Chem. Catal.* **2**, 2034–2048 (2022).
27. Zou, S., Yu, B. & Huang, H. Palladium-catalyzed ring-closing aminoalkylative amination of unactivated aminoenynes. *Angew. Chem. Int. Ed.* **62**, e202215325 (2023).
28. Hoffmann-Röder, A. & Krause, N. Synthesis and properties of allenic natural products and pharmaceuticals. *Angew. Chem. Int. Ed.* **43**, 1196–1216 (2004).
29. Ma, S. Some typical advances in the synthetic applications of allenes. *Chem. Rev.* **105**, 2829–2872 (2005).
30. Yu, S. & Ma, S. Allenes in catalytic asymmetric synthesis and natural product syntheses. *Angew. Chem. Int. Ed.* **51**, 3074–3112 (2012).
31. Adams, C. S., Weatherly, C. D., Burke, E. G. & Schomaker, J. M. The conversion of allenes to strained three-membered heterocycles. *Chem. Soc. Rev.* **43**, 3136–3163 (2014).
32. Alcaide, B. & Almendros, P. Novel cyclization reactions of aminoallene. *Adv. Synth. Catal.* **353**, 2561–2576 (2011).
33. Muñoz, M. P. Silver and platinum-catalysed addition of O–H and N–H bonds to allenes. *Chem. Soc. Rev.* **43**, 3164–3183 (2014).
34. Luo, H., Yang, Z., Lin, W., Zheng, Y. & Ma, S. A catalytic highly enantioselective allene approach to oxazolines. *Chem. Sci.* **9**, 1964–1969 (2018).
35. Mszar, N. W., Haeffner, F. & Hoveyda, A. H. NHC–Cu-catalyzed addition of propargylboron reagents to phosphinoylimines. enantioselective synthesis of trimethylsilyl-substituted homoallenylamides and application to the synthesis of S-(−)-Cycloooidin. *J. Am. Chem. Soc.* **136**, 3362–3365 (2014).
36. Zhou, W. et al. A bridged backbone strategy enables collective synthesis of strychnan alkaloids. *Nat. Chem.* **15**, 1074–1082 (2023).
37. Qiu, H. et al. A Bischler–Napieralski and homo-Mannich sequence enables diversified syntheses of sarpagine alkaloids and analogues. *Nat. Commun.* **14**, 5560 (2023).
38. Chu, W.-D., Zhang, Y. & Wang, J. Recent advances in catalytic asymmetric synthesis of allenes. *Catal. Sci. Technol.* **7**, 4570–4579 (2017).
39. Cowen, B. J., Saunders, B. S. & Miller, J. Pyridylalanine (pal)-peptide catalyzed enantioselective allenoate additions to N-acyl imines. *J. Am. Chem. Soc.* **131**, 6105–6107 (2009).
40. He, Z. & Yudin, A. K. A versatile synthetic platform based on strained propargyl amines. *Angew. Chem. Int. Ed.* **49**, 1607–1610 (2010).
41. Hashimoto, T., Sakata, K., Tamakuni, F., Dutton, M. J. & Maruoka, K. Phase-transfer-catalysed asymmetric synthesis of tetrasubstituted allenes. *Nat. Chem.* **5**, 240–244 (2013).
42. Poh, J.-S. et al. Rapid asymmetric synthesis of disubstituted allenes by coupling of flow-generated diazo compounds and propargylated amines. *Angew. Chem. Int. Ed.* **56**, 1864–1868 (2017).
43. Kondo, M., Omori, M., Hatanaka, T., Funahashi, Y. & Nakamura, S. Catalytic enantioselective reaction of allenylnitriles with imines using chiral bis(imidazoline)s palladium(II) pincer complexes. *Angew. Chem. Int. Ed.* **56**, 8677–8680 (2017).
44. Hölzl-Hobmeier, A. et al. Catalytic deracemization of chiral allenes by sensitized excitation with visible light. *Nature* **564**, 240–243 (2018).
45. Cui, Y. et al. Chirality memory of α-methylene-π-allyl iridium species. *Chem. Sci.* **12**, 11831–11838 (2021).
46. Trost, B. M., Fandrick, D. R. & Dinh, D. C. Dynamic kinetic asymmetric allylic alkylations of allenes. *J. Am. Chem. Soc.* **127**, 14186–14187 (2005).
47. Wan, B. & Ma, S. Enantioselective decarboxylative amination: synthesis of axially chiral allenes. *Angew. Chem. Int. Ed.* **52**, 441–445 (2013).
48. Li, Q., Fu, C. & Ma, S. Palladium-catalyzed asymmetric amination of allenyl phosphates: enantioselective synthesis of allenes with an additional unsaturated unit. *Angew. Chem. Int. Ed.* **53**, 6511–6514 (2014).
49. Zha, T. et al. Direct catalytic asymmetric and regiodivergent N_1- and C_3-allenylic alkylation of indoles. *Angew. Chem. Int. Ed.* **62**, e202300844 (2023).
50. Adamson, N. J., Jeddi, H. & Malcolmson, S. J. Preparation of chiral allenes through Pd-catalyzed intermolecular hydroamination of conjugated enynes: enantioselective synthesis enabled by catalyst design. *J. Am. Chem. Soc.* **141**, 8574–8583 (2019).
51. Li, Q., Fang, X., Pan, R., Yao, H. & Lin, A. Palladium-catalyzed asymmetric sequential hydroamination of 1,3-enynes: enantioselective syntheses of chiral imidazolidinones. *J. Am. Chem. Soc.* **144**, 11364–11376 (2022).
52. Ruiz-Castillo, P. & Buchwald, S. L. Applications of palladium-catalyzed C–N cross-coupling reactions. *Chem. Rev.* **116**, 12564–12649 (2016).
53. Ogasawara, M. et al. Synthesis, structure, and reactivity of (1,2,3-η^3-butadien-3-yl)palladium complexes. *Organometallics* **26**, 5025–5029 (2007).
54. Hiesinger, K., Dar'in, D., Proschak, E. & Krasavin, M. Spirocyclic scaffolds in medicinal chemistry. *J. Med. Chem.* **64**, 150–183 (2021).
55. Xu, P.-W. et al. Catalytic enantioselective construction of spiro quaternary carbon stereocenters. *ACS Catal.* **9**, 1820–1882 (2019).
56. Carreras, J., Avenoza, A., Busto, J. H. & Peregrina, J. M. Ring-rearrangement metathesis of 1-substituted 7-azanorbornenes as an entry to 1-azaspiro[4.5]decane systems. *J. Org. Chem.* **76**, 3381–3391 (2011).

57. Burés, J. Variable time normalization analysis: general graphical elucidation of reaction orders from concentration profiles. *Angew. Chem. Int. Ed.* **55**, 16084–16087 (2016).
58. Gumrukcu, Y., de Bruin, B. & Reek, J. N. H. Hydrogen-bond-assisted activation of allylic alcohols for Palladium-catalyzed coupling reactions. *ChemSusChem* **7**, 890–896 (2014).
59. Jagushte, K. U., Sadhukhan, N., Upadhyaya, H. P. & Choudhury, S. D. Dual excited state proton transfer pathways in the bifunctional photoacid 6-amino-2-naphtol. *J. Phys. Chem. B* **127**, 9788–9801 (2023).
60. Hartwig, J. F. Electronic effects on reductive elimination to form carbon–carbon and carbon–heteroatom bonds from palladium(II) complexes. *Inorg. Chem.* **46**, 1936–1947 (2007).
61. Kazmaier, U. *Transition Metal Catalyzed Enantioselective Allylic Substitution in Organic Synthesis* (Springer, 2012).
62. Crabtree, R. H. Deactivation in homogeneous transition metal catalysis: causes, avoidance, and cure. *Chem. Rev.* **115**, 127–150 (2015).
63. Frings, M., Bolm, C., Blum, A. & Gnamm, C. Sulfoximines from a medicinal chemist's perspective: physicochemical and in vitro parameters relevant for drug discovery. *Eur. J. Med. Chem.* **126**, 225–245 (2017).
64. Zheng, Y., Tice, C. M. & Singh, S. B. The use of spirocyclic scaffolds in drug discovery. *Bioorg. Med. Chem. Lett.* **24**, 3673–3682 (2014).
65. Lovering, F., Bikker, J. & Humblet, C. Escape from flatland: increasing saturation as an approach to improving clinical success. *J. Med. Chem.* **52**, 6752–6756 (2009).
66. Noji, S. et al. Discovery of a janus kinase inhibitor bearing a highly three-dimensional spiro scaffold: JTE-052 (delgocitinib) as a new dermatological agent to treat inflammatory skin disorders. *J. Med. Chem.* **63**, 7163–7185 (2020).
67. Garnsey, M. R. et al. Discovery of the potent and selective MC4R antagonist PF07258669 for the potential treatment of appetite loss. *J. Med. Chem.* **66**, 3195–3211 (2023).
68. Xiang, W. et al. Discovery of ARD-1676 as a highly potent and orally efficacious AR PROTAC degrader with a broad activity against AR mutants for the treatment of AR+ human prostate cancer. *J. Med. Chem.* **66**, 13280–13303 (2023).

Acknowledgements

The authors are grateful for the financial support by the National Natural Science Foundation of China (21925111, 92356302, 22301290, 22301289, and 22350008), the Strategic Priority Research Program of the Chinese Academy of Sciences (XDB0450301) and the National Key R&D Program of China (2021YFA1501003, 2023YFA1507500) (H.H.). This work was partially carried out at the Instruments Center for Physical Science, University of Science and Technology of China.

Author contributions

H.H. conceived the concept and directed the project. S.Z., Z.Z., and G.Y. conducted the experiments. S.Z. and H.H. wrote the paper. All the authors discussed and analyzed the results and commented on the manuscript.

Competing interests

The authors declare no competing interests.

Additional information

Supplementary information The online version contains supplementary material available at https://doi.org/10.1038/s41467-024-54328-5.

Correspondence and requests for materials should be addressed to Hanmin Huang.

Peer review information *Nature Communications* thanks the anonymous reviewer(s) for their contribution to the peer review of this work. A peer review file is available.